AJDS LAZHAR Al-Azhar Journal of Dental Science Print ISSN 1110-6751 | online ISSN 2682 - 3314
Vol. 26- No. 4- 517:530- October 2023 https://ajdsm.journals.ekb.eg
Oral Biology, Medicine & Surgical Sciences Issue *(Oral Biology, Oral Pathology, Oral Periodontology, Medicine, Oral & Maxillofacial Surgery)*

THERAPEUTIC POTENTIAL OF EPIGALLOCATECHIN-3-GALLATE ON CANCER STEM CELLS OF DMBA INDUCED HAMSTER BUCCAL POUCH CARCINOMA

Mohamed Alaa Al-Dosoki[1*], Ahmed Abd-Alshakor Abd-Alhafez [2], Asmaa Mohamed Zahran[3], Mohamed Gomaa Attia Zouair[4]

ABSTRACT

Objective: The aim of the present study was directed to investigate the therapeutic potential of epigallocatechin-3-gallate (EGCG) on cancer stem cell(s) (CSC(s)) of DMBA induced hamster buccal pouch (HBP) carcinoma. **Subjects and methods:** thirty Syrian male hamsters were divided into three group(s) (G(s)),10 each. GI: negative control, left untreated. The right pouches of those in GII and GII were painted with DMBA (3times /a week/ 14 weeks). GII: positive control, not received other treatment. GIII was injected with intraperitoneally with EGCG. After termination of the experiment, gross observations were recorded, then, the animals were euthanized, all pouches were surgically excised and bisected. The first piece was prepared, fixed and processed for hematoxylin and eosin (H&E) stain examination and immunohistochemical (IHC) staining utilizing CD44 and CD24. The other piece of the fresh tissue was used for flow cytometric (FCM) assessment for identification of CSCs using CD44&CD24 fluorophore-antibodies, then, apoptosis assay of the identified CD44+CD24- CSCs was employed. **Results:** the results of GIII revealed some variability compared to those observed in GII in gross observations as well as when utilizing H&E stain, CD44 & CD24 IHC and FCM assessment of CSCs. CD44 &CD24 IHC revealed highly significant difference between GII and GIII, (p value > 0.001). CSCs identification, CD44+CD24-& CD44+CD24+revealed highly significant difference between GII and GIII, (p value > 0.05)}. The CD44+CD24- CSCs apoptosis recorded highly significant difference between GII and GIII (p value < 0.001). **Conclusion:** EGCG significantly inhibits tumor progression and induces apoptosis in CSC of HBP carcinoma.

KEY WORDS: CSC, EGCG, HBP carcinoma.

INTRODUCTION

Oral carcinogenesis is a multistage, multi-mechanism carcinogenesis process, comprising mutagenic, cell death and epigenetic mechanisms, through three separates but closely linked stages: initiation, promotion, and progression. The chief reason of the initiation phase is a solitary applying of a subcarcinogenic dose of a carcinogen. In another words, exposing to carcinogen agents that creates eternal injuries to inherited material, which

1. Assistant Lecturer, Oral and Dental Pathology Department, Faculty of Dental Medicine (Boys- Cairo), Al-Azhar University, Egypt.
2. Lecturer, Oral and Dental Pathology Department, Faculty of Dental Medicine (Boys- Cairo), Al-Azhar University, Egypt.
3. Professor, Department of Clinical Pathology, South Egypt Cancer Institute, Assiut University, Egypt.
4. Professor, Oral and Dental Pathology Department, Faculty of Dental Medicine (Boys-Cairo), Al-Azhar University, Egypt.

• ***Corresponding author*:** mohamedalaa.9@azhar.edu.eg

DOI: *10.21608/AJDSM.2021.109599.1276*

are almost irreversible. Promotion, the second step, resulted via repeatedly applying of an irritating agent. It involves cellular explosion and choosy clonal growth which are reversible, during its primal phases, but becomes unredeemable with time[1, 2].

It has been established that, oral carcinogenesis brought by-dimethylbenz (a) anthracene (DMBA) in golden Syrian hamsters is an accepted and well honored experimental example for memorizing biochemical, histopathological, immunohistochemical (IHC) and molecular modification[3]. Unfortunately, oral squamous cell carcinoma (OSCC) is associated with high morbidity and mortality. Although, great progress has been made in diagnosis and treatment strategies, the 5-year survival rate of OSCC sufferers remains disappointingly low, which is mainly attributed to the poor drug efficacy, metastatic spread and resistance[4, 5].

An arising conception of carcinogenesis proposes that CSCs sit atop of a miscellaneous population of cells within cancer and are defined functionally as a subset of cells that display sternness characteristics, including the capability to asymmetrically branch, resulting in self-renewal of CSCs and the production of heterogeneous populations of cancer cells [6]. CSCs are largely tumorigenic compared to the different cancer cells and are supposed to be broadly dependable for the natural characteristics of cancer, namely, rapid growth, invasion, and metastasis. CSCs also show a greater capacity for migration, invasion, proliferation in vitro[7] and they induce far larger growths in immunocompromised xenograft mice with fewer transplanted cells compared to large numbers of unsorted cancer cells [8]. Thus, targeted curatives and diagnostics engaging CSCs are regarded a peculiar and hopeful choosing for effective cancer treatment through the targeting of tumor definite features[9].

It's accepted that, plant derived-natural outcomes have been under observation in recent times in battle of cancer cure [10, 11]. Due to the capability of phytochemicals in apoptosis initiation, cell cycle arrest, metastasis inhibition and multitargeting capacity, they are able to inhibit cancer progression[12, 13]. Among them, epigallocatechin-3-gallate (EGCG(which is a natural product, was introduced to be the most abundant catechin in green tea[14]. EGCG attracted significant research interest due to its beneficial health effects including anti-oxidation[15] and anti-tumorigenesis activity[16]. EGCG inhibit CSCs of the breast, lung, prostate and liver, CSCs are targets of EGCG for cancer prevention and therapy[17]. Commixing EGCG with cisplatin or oxaliplatin deepened the curative effect in human colorectal cancer cells [18].

The main objective for the present study was to assess the therapeutic potential of EGCG on CSCs of DMBA induced hamster buccal pouch (HBP) carcinoma. The assessment based on the animal's general health examinations, HBP gross observations, histological tumor tissue changes, IHC examinations and flow cytometric (FCM) studies.

SUBJECTS AND METHODS

Chemicals: DMBA (0.5%) was obtained from Sigma-Aldrich Company, dissolved in paraffin oil. EGCG (E4268) were purchased from Sigma Aldrich Company, prepared by direct dissolving the crystalline compound in 0.9% sodium chloride injection (10 mg/ml).

Animals: thirty Syrian male hamsters five weeks old, weighing 80-120g were obtained from the animal house, Cairo University, Cairo, Egypt. The experimental animals were housed in standard coops with sawdust coverlet under managed environmental conditions of moistness (30-40%), temperature (20 ± 2°C), and light (12-h light/12-h dark). All experimental animals were supplied with standard diet and water ad libitum.

Sample size: Based on Duzgun et al (2017) research[19], a sample size of 10 in each group, in the current study, had a 80% power to detect a difference between means of 0.53 with a significance level

(alpha) of 0.05 (two-tailed) at 95% confidence intervals. In 80% (the power) of those experiments, the p value was less than 0.05 (two-tailed) so the results were deemed "statistically significant". In the remaining 20% of the experiments, the difference between means was deemed "not statistically significant". Report created by GraphPad StatMate 2.00.

Experimental design: After a week of adaptation, the animals were divided randomly into three group$_{(s)}$ ($G_{(s)}$), 10 each. While the animals in GI (negative control) were left untreated, the right pouches of those in GII and GIII were painted with the 0.5% DMBA in liquid paraffin using a number 4 camel's hair brush, 3 times a week for 14 weeks[20]. After that, the animals in GII (positive control) not received other treatment while those in GIII (EGCG) were injected intraperitoneally with EGCG (10mg/kg / twice a week/ 4 weeks).

General health examinations: during the trial, the changes in the animal's general health were recorded. Hamsters appeared one or further of these characters if they were shifting with disease or injury loss of eagerness, quiescence, piling in a corner, sneezing, hyperventilating, and/ or discharge from the nose or eyes, moistness around the tail, diarrhea and hair extinction.

After termination of the experiment, gross observations were recorded (mucosal thickness, exudation, ulcers, and tumors.), the animals were euthanized, the right cheek pouch everted, and the diameter of each tumor was measured with a Vernier caliper. The tumor volume was calculated by the formula, Vmm3 = (4/3) π [(D1/2) (D2/2) (D3/2)], where D1, D2 and D3 are the three diameters (mm) of the tumor[21]. Then, the right cheek pouch was excised and bisected with one piece of the fresh tissue in saline in order to be examined by FCM and the other piece of the fresh tissue, fixed in 10% neutral buffered formalin, routinely processed and embedded in paraffin blocks in order to be examined histologically and immunohistochemically.

Histopathological examinations: the fixed specimens were dehydrated in an ascending ethanol series, embedded in paraffin wax to form paraffin blocks. Tissue sections of 4μm thickness were cut using rotary microtome, mounted on glass slides, processed, and stained with hematoxylin and eosin (H&E) for light microscopic examination.

Measurement of the depth of invasion (DOI): DOI was measured for all surgical specimens based on the H&E slide. DOI was measured from the basal layer of the surface epithelium to the deepest point of tumor invasion. It has further been classified as less invasive ≤5 mm, moderate invasive 6–10 mm, and deeply invasive ≥10 mm, according to American Joint Committee on Cancer (AJCC)[22] **.** DOI was measured using Leica QWIN V3 image analyzer computer system (Switzerland), controlled by Leica QWIN V3 software. This was done in Oral and Dental Pathology Department, Faculty of Dental Medicine (Boys-Cairo), Al-Azhar University, Egypt.

Immunohistochemical examination: Other tissue sections were cut at 4μm and put on positive charged slides for the application of standard labeled streptavidin- biotin method to demonstrate the expression of CD44 & CD24 antibodies. The sections were deparaffinized in xylene and rehydrated through graded ethanol (100%, 95% and 70%) each run for 5 minutes. Slides were washed in distilled water then in phosphate buffered saline (PBS), each for 5 minutes. Endogenous peroxidase activity was blocked using 3% solution of hydrogen peroxide (H_2O_2) in methanol for 30 minutes at room temperature. Slides were then washed in PBS. Slides were then immersed in plastic jars containing 200 ml of citrate buffer (pH6). The jars were put in microwave at maximum power at 100°C for 3 intervals, each one 5 minutes. Slides were left at room temperature to coal gradually. Slides were then washed in distilled water followed by PBS for 5 minutes. Tissue sections were received

one or two drops of the primary antibodies (CD44 or CD24) in a dilution of 1:100 and incubated in a humid chamber at room temperature overnight. Slides were then washed in distilled water, followed by PBS for 5 minutes. Biotinylated secondary antibody was added and incubated at room temperature for 30 minutes. Tissue sections were then washed in PBS for 5 minutes. One or two drops of peroxidase-labeled streptavidin were applied for 30 minutes at room temperature then washed in PBS. The tissue sections were received DAB for 2-4 minutes to develop color, followed by putting in distilled water. Tissue sections were counterstained using Mayer's hematoxylin for one minute and then washed in tap water. The slides were placed in two changes of 95% alcohol followed by two changes of absolute alcohol, each for 3 minutes then mounted with DPX and covered with plastic covers in order to be examined. Negative controls were prepared by omitting the primary antibody. Spleen tissues were used as positive controls for both antibodies[23].

The immunostained sections were examined using light microscope to assess the prevalence of positive cases and the localization of immunostaining within the tissues. In addition, image analysis computer system was used to assess area percentage of the positive cells of the immunostaining. This was done in Oral and Dental Pathology Department, Faculty of Dental Medicine (Boys-Cairo), Al-Azhar University, Egypt.

Flow cytometric detection and identification of CSCs

Mechanical dissociation of OSCC: the tumor mass was placed into a 35 mm petri dish with 3 mL of PBS. Tumor specimen was extensively washed (2 to 3 times) in PBS to remove blood and debris. The specimen was held firm with tissue forceps, and using the back of a number 22 scalpel blade, the specimen was scraped downward, and away, such that cells are pulled off the tumor mass into the dish. As cells were broken from the tumor mass, strands of connective tissue (CT) were isolated, and were removed from the collection. The scrapping was continued until the specimen is too small to hold to have a large population in the dish. The tumor solution was pipetted up and down 3 to 5 min with a 5-ml disposable pipet. Then, the solution was placed into a 15-ml conical tube. The remaining sample was centrifuged at 2500 rpm for 2 minutes at 4°C. The media was aspirated off and the cellular pellet was resuspended in PBS in an appropriate volume needed for FCM analysis[24].

Identification of CSCs: the cellular pellet was suspended in PBS in an appropriate volume. 10 µL of PE-CD24, 10 µL APC-CD44, annexin V and PI were added to the sample. The samples were incubated with the antibodies for 30 minutes at 4°C, protected from light. The cells were resuspended in PBS and acquired 50000 cells by FACSCalibur flow cytometer (BD Biosciences) with BD FACSDiva 7.0 software. Cell populations were identified using FACSCalibur flow cytometer. Firstly, Cells were gated based on light scatters, then by positive gating of CD44+ CD24- and CD44+ CD24+ cells, then CD44+ CD24- were further gated for analysis of apoptosis[25]. This was done in the FCM Unit, Clinical Pathology Department, South Egypt Cancer Institute, Assiut University, Egypt.

Statistical analysis

The results were recorded as the mean ± standard deviation (SD) and statistically analyzed. A one-way analysis of variance (ANOVA) was performed using SPSS version 17.0 for windows. The comparison between more than two independent groups with quantitative data and parametric distribution was done by using ANOVA followed by post hoc analysis using LSD test. The p value was considered significant as the following: $p>0.05$: non-significant, $p<0.05$: significant and $p<0.001$: highly significant.

RESULTS

Gross observations and tumor volume: GI showed good generalized health with no gross changes, no hair loss, no skin ulcerations, normal pale pink color of the HBP with neither pathological nor inflammatory changes. Their buccal pouch lengths were about 5cm for all hamsters **(Fig.1A)**. GII showed marked hair loss, pouch depth decrease, skin ulcers and marked debilitation of all animals. Animal's pouches showed large exophytic growths with pronounced vascularity and the pouch length ranged from 1.5-2cm with distal necrotic end. Using vernier caliper, the mean tumor volume of tumor-bearing animals was 779.5 mm^3 **(Fig.1B)**. GIII showed slight improvement in the general health. The length of the pouches was about 2.5cm with reduction of distal necrosis. Slight decrease in size of the papillomatous lesions was observed. Using vernier caliper, the mean tumor volume of tumor-bearing animals for GIII was 409.5 mm^3 **(Fig.1C)**.

Histopathological and immunohistochemical results: GI revealed normal thin stratified squamous epithelium, consists of two to four layers of squamous cells exhibiting slight keratinization; one layer of basal cells and one, two or three layers of spinous and thin keratinized cells with lacking rete ridges. Sub-epithelial CT and muscular layer were seen **(Fig.2A)**. The IHC staining using CD44 antibody exhibited positive membranous expression (mean = 35.4%) which limited to basal and suprabasal layers **(Fig.2B)** while the CD24 expression showed positive membranous expression (mean = 0.3%) which present in the upper layers of normal epithelium **(Fig.2C)**. GII revealed well to moderate differentiated SCC in the form of large papillomatous lesions with invading islands of epithelium into underlying C.T (DOI=10.7mm) with marked chronic inflammatory cells and necrotic mass at the distal end of pouch. The invading epithelial cells showed basal cell hyperplasia, loss of basal cells polarity, hyperchromatism, prominent nucleoli, altered N\C ratio, swirling of spinous layer and cellular & nuclear pleomorphism **(Fig.2D)**. The IHC staining using CD44 exhibited positive membranous-cytoplasmic expression (mean=65.51%) throughout the epithelial layers and invading tumor cells **(Fig.2E)** while CD24 (positive in 8 samples and negative in 2 samples) exhibited positive membranous-cytoplasmic expression (mean=68.6%) throughout the epithelial layers and invading tumor cells **(Fig.2F)**. GIII revealed moderate to severe epithelial dysplasia with areas of top to bottom changes or carcinoma

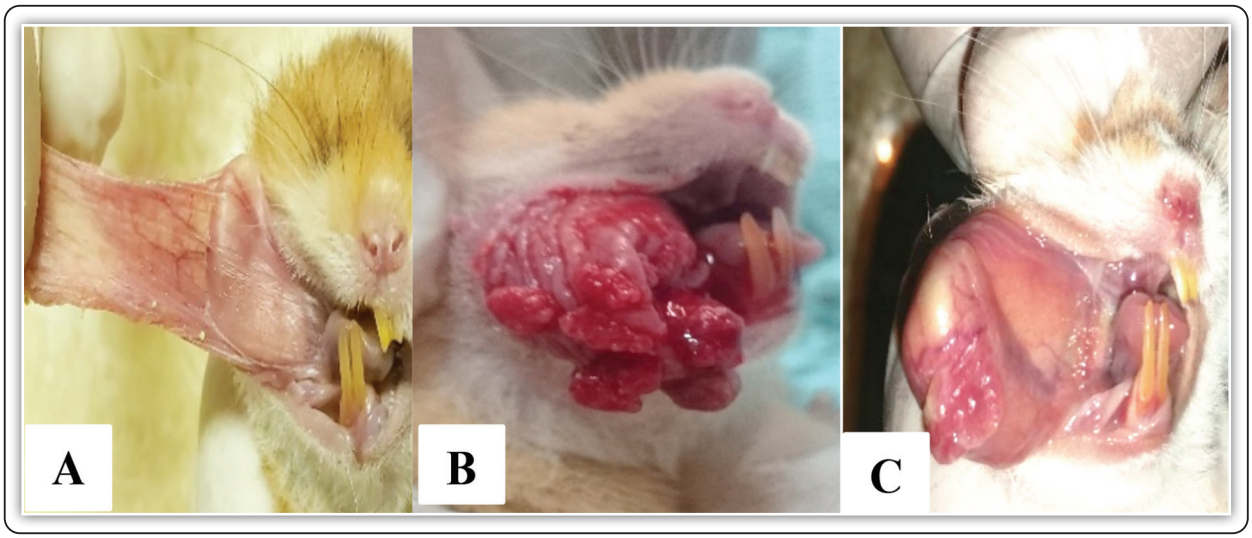

FIG (1) **A:** HBP of GI showing normal buccal pouch mucosa, which appeared pink in color with smooth surface (arrow). **Fig.1B:** HBP of GII showing multiple exophytic papillary tumor masses surrounded with bleeding areas (arrow). **Fig.1C:** HBP of GIII showing small size nodule with absence of ulceration and bleeding (arrow).

in situ (CIS)were seen in five hamsters while the other five hamsters showed superficial invasion of malignant cells in the form of well differentiated SCC which was limited to the nodules only, not extended to deeper areas (DOI=1.8mm). There was reduction of the distal necrosis, inflammatory infiltration and increase amount of collagen fibers (**Fig.2G**). The IHC staining using CD44 exhibited positive membranous-cytoplasmic expression (mean= 50.76%) throughout the epithelial layers and invading tumor cells **(Fig.2H)** while CD24 (positive in 5 samples and negative in 5 samples) exhibited positive membranous-cytoplasmic expression (mean=33.3%) throughout the epithelial layers and invading tumor cells **(Fig.2I)**.

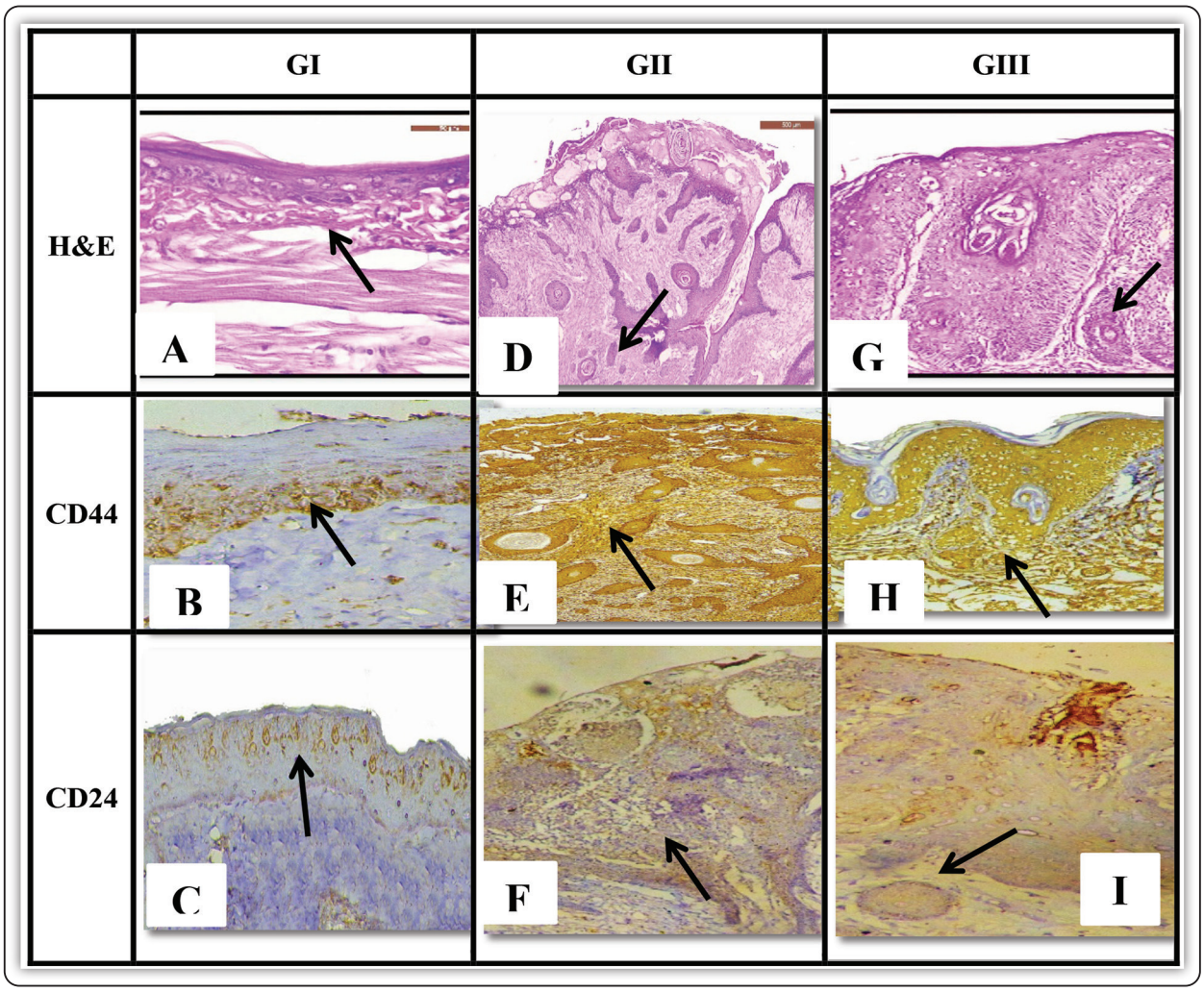

FIG (2) **Fig.2A:** H&E stain of GI showing keratinized stratified squamous epithelium with flattened rete ridges, sub-epithelial CT layer and muscular layer (arrows). **Fig.2B:** IHC expression of CD44 showing positive membranous expression which limited to basal and suprabasal layers (arrow). **Fig.2C:** IHC expression of CD24 positive membranous expression which present in the upper layers of normal epithelium (arrow). **Fig.2D:** H&E stain GII showing well differentiated SCC with deep invasion of multiple tumor islands into the underlying CT (arrows). **Fig.2E:** IHC expression of CD44 showing positive membranous-cytoplasmic expression throughout the epithelial layers and invading tumor cells (arrow). **Fig.2F:** IHC expression of CD24 showing positive membranous-cytoplasmic expression throughout the epithelial layers and invading tumor cells (arrow). **Fig.2G:** H&E stain of GIII showing well differentiated SCC (superficial invasion) (arrow). (H&E stain X400) (arrows). **Fig.2H:** IHC expression of CD44 positive membranous-cytoplasmic expression throughout the epithelial layers and invading tumor cells (arrows). **Fig.2I**: IHC expression of CD24 showing positive membranous-cytoplasmic expression throughout the epithelial layers and invading tumor cells (arrows).

Statistical analysis results of tumor volume and CD44 & CD24 expression:

Tumor volume: There was highly significant difference between GII and GIII (p value < 0.001) **(Table.1, Fig.3).**

CD44: statistical analysis results revealed that, GI had recorded the lowest mean area percentage (35.4%), while GII had the highest mean area percentage (65.1 %). There was highly significant difference between GI& GII (p value <0.001). There was significant difference between GII & GIII (p value = 0.002 respectively) **(Table.1, Fig .4).**

CD24: statistical analysis results revealed that, GI had recorded the lowest mean area percentage (0.3%), while GII had the highest mean area percentage (68.6 %). There was highly significant difference between GI& GII (p value<0.001). There was highly significant difference between GII and GIII (p value < 0.001) **(Table.1, Fig .4).**

Correlation analysis: there was a statistically high significant positive (direct) correlation either between CD44 and CD24 or between tumor volume and area percentage of CD44 & CD24 expressions (p value > 0.001) (Table.2, Fig.5). This means that an increase in one variable is associated with an increase in the other variable and vice versa.

TABLE (1) Comparison between studied groups as regard to tumor volume and CD44 & CD24 expressions.

		GI (n = 10)	GII (n = 10)	GI11 (n = 10)	F	P-value
Tumor volume	**Mean**	-----	779.5	409.5	**144.9**	**< 0.001 HS**
	±SD	-----	121.3	71.2		
CD44	**Mean**	35.4	65.51	50.76	**11.02**	**< 0.001 HS**
	±SD	12.6	13.3	12.2		
CD24	**Mean**	0.3	68.6	33.3	**180.7**	**< 0.001 HS**
	±SD	0.7	8.9	6.2		

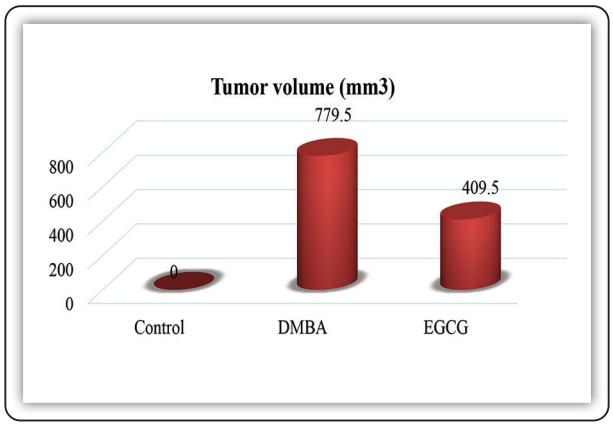

FIG (3) Bar chart representing tumor volume in the studied groups.

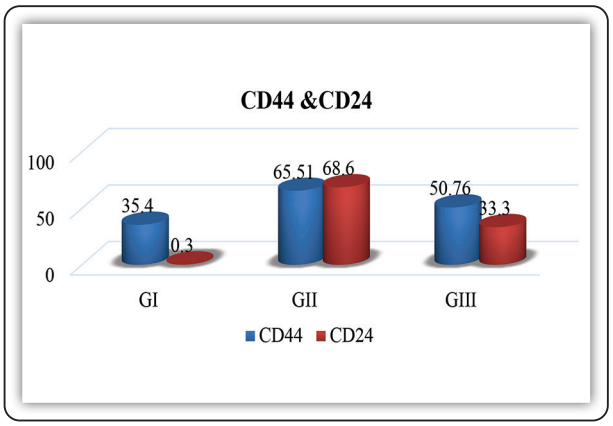

FIG (4) Bar chart representing nean area% results of CD44&CD24 experssions.

TABLE (2) Correlation of tumor volume and CD44 & CD24 expressions.

	Tumor volume	
	Correlation coefficient (r)	p-value
Area % of CD44	**0.636**	**> 0.001**
Area % of CD24	**0.595**	**> 0.001**

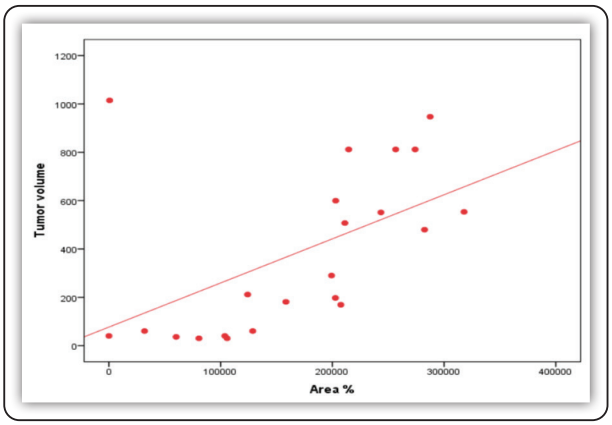

FIG (5) Correlation of tumor volume and area % of CD44 &CD24 expressions.

Identification of CSCs: two phenotypic subpopulations were separated, CD44+/CD24- and CD44+/CD24+. The percentage of CD44+/CD24- cells in GI, GII and GIII was 0.005%, 1.33%, and 0.28% respectively. While the percentage of CD44+/CD24+ cells in GI, GII and GIII was 0.001%,0.11% and 0.04% respectively. There was highly significant difference between GI& GII (p value < 0.001). There was highly significant difference between GII and GIII (p value > 0.05). (Table.3, Fig .6).

TABLE (3) Comparisons between studied groups as regard CD44+ CD24- & CD44+CD24+ and apoptosis of CD44+ CD24-CSC.

		GI (n = 10)	GII (n = 10)	GIII (n = 10)	F	P-value
CD44+ CD24-	**Mean**	0.005	1.33	0.28	**159.4**	**< 0.001 HS**
	±SD	0.002	0.21	0.07		
CD44+ CD24+	**Mean**	0.001	0.11	0.04	**26.2**	**< 0.001 HS**
	±SD	0.002	0.04	0.01		
Apoptosis of CD44+ CD24-CSC	**Mean**	0.0	1.3	21.8	**15.8**	**< 0.001 HS**
	±SD	0.0	0.7	7.3		

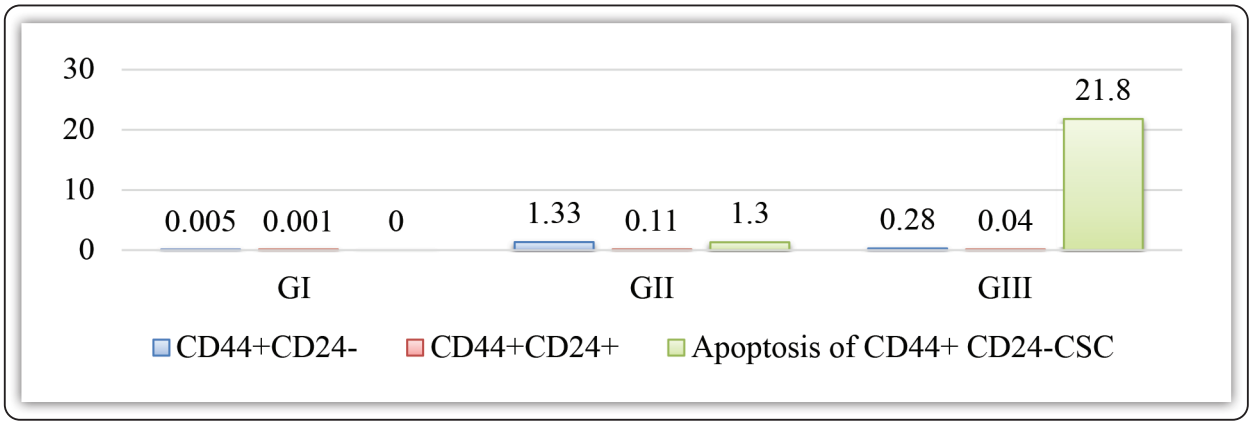

FIG (6) Bar chart representing mean results of CD44+ CD24- and CD44+ CD24+.

Apoptosis assay of CD44+CD24- CSCs: GII, 1.3% of the cells underwent apoptosis while the cells of GIII resulted in 21.8% apoptosis. There was highly significant difference between GII and GIII (p value <0.001). (Table.3, Fig .6).

DISCUSSION

To our knowledge, in the liberal English literatures, this was the foremost research to estimate the therapeutic potential of EGCG on CSCs of DMBA induced HBP carcinoma. The results of animal's general health examinations, HBP gross observations, H&E stain and IHC examinations utilizing antibodies against CD44 and CD24 CSCs markers, revealed variable observations.

In the present study, GI showed no observable abnormalities of the HBP with neither pathological nor inflammatory changes. After animal's euthanization, the buccal pouches length was about (5cm) for all hamsters with normal histological structures. Bruna et al (2017)[26], reported the same finding. IHC staining of GI showed positive membranous expression of CD44 (35.4%) that was seen to be restricted to the basal and supra-basal layers and almost negative in the remaining epithelial cell layers. This result is in accordance with that of additional investigators[27,28]. This observation might be attributed to that, CD44 expression in the normal epithelium indicates that, CD44 is needed for the conservation of epithelial architecture as a total by the homing of the epithelial cells. Williams et al (2013)[29] stated that, CD44 synthesizes matrix molecules and interacts with a mass of elements to manage lineage specification, discrimination, stem cell survival, self-renewal, cell migration, cell–cell adhesion and growth factor receptor signaling. IHC staining of GI showed positive membranous expression of CD24 (0.3 %) that was seen in the upper, more differentiated layers of normal epithelium rather than the supposed stem cell niche in the basal layer. This result is in agreement with that of other investigators [30,31]. Weichert et al (2005)[31] stated that, CD24 is a small glycosylated, cell exterior protein that's manifested physiologically in the growing up pancreas, brain, reawakening muscle, normal keratinocytes and renal tubules. Its physiologic purpose is not detailed clarified, but it seems to be enclosed in control of cell expansion, apoptosis, and cell attachment.

In the current study, GII showed marked debilitation of all animals. Animal's pouches showed large exophytic growths with pronounced vascularity. The mean tumor volume of tumor-bearing animals was 779.5mm3 and 100% tumor formation. The pouch length (1.5-2cm) which decreased compared to GI due to necrosis in the distal end of the pouch. These observations are mainly due to the strong toxic DMBA effect[32]. By using H&E stain, a development of various patterns of invasive SCC 100% (well differentiated and moderately differentiated) were seen which extended to deeper areas of C.T (DOI=10.7mm). These observations might be attributed to DMBA induced over production of ROS, chronic inflammation, oxidative modification of DNA bases, impairment in antioxidant defense system, defect in the activities of detoxification cascade and deregulated expression pattern of molecular markers are implicated in the promotion and progression of oral carcinogenesis[33].

In the current study, IHC staining of GII showed positive membranous-cytoplasmic expression of CD44 (65.51%) that was seen throughout the epithelial layers and invading tumor cells, that showed highly significantly expression compared to GI (p value < 0.001). This result is in agreement with that of other investigators[34, 35]. Paulis et al (2015)[35] concluded that, CD44 expression escalated the assaultiveness of tumor cells behavior. On the other hand, Margaritescu et al (2011)[36] showed a limited usefulness of CD44 expression in identifying the CSCs in OSCCs. This shortening in the role of the CD44 may be due to improper selection of the examined tissues, which may have massive areas of inflammation leading to a false result in expression of the CD44. Moreover, the difference in the

sorting techniques, than the IHC, for identification the CD44 expression in tissue as western blotting and flow cytometric assessments may demonstrate different results.

In the present study, IHC staining of GII showed positive membranous-cytoplasmic expression of CD24 (68.6%) that was seen throughout the epithelial layers and invading tumor cells, that showed highly significantly expression compared to GI (p value < 0.001). CD24 showed positive expression in 8 samples and negative in 2 samples. This result is in agreement with that of other investigators[37,38]. Yang et al (2017)[39] found that, in human nasopharyngeal carcinoma cell lines, cells with higher CD24+ expression have increased growth and tumor sphere formation in vitro.

In the current study, the percentage of CD44+/CD24- and CD44+/CD24+ cells in GII were 1.33% and 0.11% respectively, with highly significant difference between GII and GI (p value < 0.001). This is in consistence with that shown by other studies[25,40,41]. Ghuwalewala et al (2016)[40] revealed that, CD44+CD24- cells is able to form larger spheres than CD44+CD24+within a few days, indicative of its ability to undergo asymmetric division. CD44 CD24- cells were actually, more mobile and invasive under in vitro circumscriptions. Although these cells did not expand any quick, despite altered cell cycle, but under clonal affections, could give rise to holoclone- analogous communities, a typical hallmark of stem cells with extensive differentiation potential. Conversely, Han et al (2014)[25] found that, CD24+/CD44+ cells were more proliferative and invasive in vitro and more tumorigenic in vivo forming larger tumors in immunodeficient mice equated to its carbon copyCD24-/CD44+ cells. In addition, CD24+/CD44+ cells were scarcely more resistant to chemotherapeutic agencies likened to CD24-/CD44+ cells.

By FCM, the current study revealed that, only 1.3% of CD44+CD24- CSCs undergo apoptosis with highly significant expression compared to GI (p value < 0.001). These results are in agreement with other researchers[40-42].Todoroki et al (2016)[41] found that, anti-apoptotic genes such as Bcl-2 and CFLAR were more highly expressed in the CD44+/CD24– cells using real-time PCR assays.

In the present study, GIII showed slight improvement in the animal's general health. The pouch length (2.5cm) decreased compared to GII due to reduction of the inflammatory infiltration and distal necrosis. Slight decrease in size of the papillomatous lesions was observed. The mean tumor volume of tumor-bearing animals was 409.5mm3. These findings conflicted on H&E staining in which five hamsters revealed moderate (10%) to severe epithelial dysplasia (20%) or CIS (20%) while the other five hamsters showed superficial invasion of well differentiated SCC (50 %) which was limited to the nodules only, not extended to deeper areas (DOI=1.8mm). These results are in agreement with other studies [43-45]. Yoshimura et al (2019)[43] reported that, EGCG diminished tumor growth, induces cell cycle arrest and apoptosis in OSCC cells, resulting in antiproliferative effects in vitro and in vivo: in a mouse model, significant growth inhibition of the OSCC tumor was observed in EGCG-treated mice. Other mechanism for EGCG inhibitory effect was proposed by Rawangkan et al (2018)[46] in which EGCG inhibited PD-L1 expression in NSCLC, induced by both IFN-γ and epidermal growth factor (EGF) in addition, EGCG reduced PD-L1 mRNA expression about 30% in melanoma cells. In brief, EGCG is an alternative immune checkpoint inhibitor that inhibits PD-L1 expression.

In the present study, IHC staining of GIII showed positive membranous-cytoplasmic expression of CD44 (61.6%) that was seen throughout the epithelial layers and invading tumor cells, that showed significant difference compared to GII (p value = 0.002). This result is in agreement with that of other investigators[47,48]. Chung et al (2015)[47] found that EGCG selectively block STAT3 phosphorylation, hence inhibiting STAT3 translocation into the

nucleus. Interaction between STAT3 and NFkB was weakened in the nucleus due to the lack of pSTAT3. As a result, the expression levels of STAT3-NFkB target genes were decreased. The decreased expression levels of these target genes downregulated the CD44 expression. IHC staining of GIII showed positive membranous-cytoplasmic expression of CD24 (33.3%) that was seen throughout the epithelial layers and invading tumor cells, that showed highly significant difference compared to GII (p value < 0.001). CD24 showed positive expression in 5 samples and negative in 5 samples. This result is in agreement with that found by Mayr et al (2015)[49], EGCG reduced mRNA levels of the two stem cell-related genes CD24 and CD133, known to be associated with enhanced aggressiveness, higher tumorigenic potential and stem cell status in biliary tract cancer.

In the present study, there was a statistically significant positive (direct) correlation either between CD44 and CD24 or between tumor volume and area % of CD44 & CD24 expressions (p value > 0.001). This result was in agreement with other studies[30, 50]. Wang et al (2017)[51]found that, high CD44 and CD24 expressions were associated with more invasive tumor and poor overall survival rate. In addition, CD24 was shown to positively correlate with tumorigenesis and cancer progression in gene expression profile. Moreover, CD44+/CD24– cell lines of breast cancer have highly invasive and metastatic properties.

In the current study, the percentage of CD44+CD24- and CD44+CD24+ cells in GIII were 0.28% and 0.04% respectively with highly significant difference between GII and GIII (p value < 0.001). This is in consistence with that shown by other studies [52, 53]. Our result verify that, EGCG can target CSCs which explained by Chen et al (2012)[54] in their study on human breast CSCs, EGCG exhibit inhibitory properties of cell proliferation and mammosphere formation, suppression of CD44+CD24- cell populations and activation of AMPK signaling pathway. FCM results revealed that, OSCC treatment with EGCG resulted in higher apoptosis of CD44+/CD24- CSCs (21.8%) than GII with high significance difference between GII and GIII (p value < 0.001). This is in consistence with that shown by other studies[55, 56]. EGCG are supposed to act as potent radical scavengers, in particularized, under expanded oxidative stress conditions. additionally, they've been appeared to persuade apoptosis in several approaches, similar as modulating pro- and anti-apoptotic protein (Bax, Bcl-2, Bcl-XL) and cell cycle controller proteins (cyclins, CDKs). EGCG are also capable to target genes and proteins that are associated with cell expansion and apoptosis, involving receptor tyrosine kinases (RTKs)[57].

CONCLUSION

In conclusion, the current study demonstrated that EGCG could significantly inhibit tumor progression and induce apoptosis not only in non-CSC OSCC but also in CSC OSCC. On the other hand, CSCs can promote tumor progression either by immunoediting for CSCs that are more suitable to survive in an immunocompetent host or by establishing conditions that facilitate tumor outgrowth within the tumor immune-microenvironment. OSCC is aggressiveness and highly invasive neoplasm that have direct correlation between CD44 and CD24 expressions. Finally, EGCG as an anticancer is a promising novel targeted therapy for treating OSCC.

REFERENCES

1. Hemler M. Tetraspanin proteins promote multiple cancer stages. Nat Rev Cancer. 2014;14(1):49-60.
2. Cichocki M, Dałek M, Szamałek M, Dubowska W. Naturally occurring phenolic acids modulate TPA-induced activation of EGFR, AP-1, and STATs in mouse epidermis. Nutr Cancer. 2014;66(2):308-14.
3. Manoharan S, VasanthaSelvan M, Silvan S, Baskaran N, Singh A, Kumar V. Carnosic acid: a potent chemopreventive agent against oral carcinogenesis. Chem Biol Interact. 2010;188(3):616-22.

4. Ghantous Y, Bahouth Z, El-Naaj I. Clinical and genetic signatures of local recurrence in oral squamous cell carcinoma. Arch oral biol. 2018;95:141-48.
5. Yanamoto S, Umeda M, Kioi M, Kirita T, Yamashita T, Hiratsuka H, et al. Multicenter retrospective study of cetuximab plus platinum-based chemotherapy for recurrent or metastatic oral squamous cell carcinoma. Cancer chemother pharmacol. 2018;81(3):549-54.
6. Da Silva S, Ferlito A, Takes R, Brakenhoff R, Valentin M, Woolgar J, et al. Advances and applications of oral cancer basic research. Oral Oncol. 2011;47(9):783-91.
7. Yanamoto S, Kawasaki G, Yamada S, Yoshitomi I, Kawano T, Yonezawa H, et al. Isolation and characterization of cancer stem-like side population cells in human oral cancer cells. Oral Oncol. 2011;47(9):855-60.
8. Han J, Fujisawa T, Husain S, Puri R. Identification and characterization of cancer stem cells in human head and neck squamous cell carcinoma. BMC cancer. 2014;14(1):173.
9. Han J, Won M, Kim J, Jung E, Min K, Jangili P, et al. Cancer stem cell-targeted bio-imaging and chemotherapeutic perspective. Chem Soc Rev. 2020;49(22):7856-78.
10. Kashyap D, Tuli H, Yerer M, Sharma A, Sak K, Srivastava S, et al. Natural product-based nanoformulations for cancer therapy: Opportunities and challenges. Semin Cancer Biol. 2021;69:5-23.
11. Ashrafizadeh M, Najafi M, Makvandi P, Zarrabi A, Farkhondeh T, Samarghandian S. Versatile role of curcumin and its derivatives in lung cancer therapy. J Cell Physiol. 2020;235(12):9241-68.
12. Samec M, Liskova A, Koklesova L, Mersakova S, Strnadel J, Kajo K, et al. Flavonoids targeting HIF-1: Implications on cancer metabolism. Cancers. 2021;13(1):130.
13. Koklesova L, Liskova A, Samec M, Zhai K, Abotaleb M, Ashrafizadeh M, et al. Carotenoids in Cancer Metastasis—Status Quo and Outlook. Biomolecules. 2020;10(12):1653.
14. Koch W, Koch W, Komsta Ł, Marzec Z, Szwerc W, Głowniak K. Green tea quality evaluation based on its catechins and metals composition in combination with chemometric analysis. Molecules. 2018;23(7):1689.
15. Cavet M, Harrington K, Vollmer T, Ward K, Zhang J. Anti-inflammatory and anti-oxidative effects of the green tea polyphenol epigallocatechin gallate in human corneal epithelial cells. Mol Vis. 2011;17:533-42.
16. Xiang L, Wang A, Ye J, Zheng X, Polito C, Lu J, et al. Suppressive effects of tea catechins on breast cancer. Nutrients. 2016;8(8):458.
17. Fujiki H, Sueoka E, Rawangkan A, Suganuma M. Human cancer stem cells are a target for cancer prevention using (−)epigallocatechin gallate. J Cancer Res Clin Oncol. 2017;143(12):2401-12.
18. Hu F, Wei F, Wang Y, Wu B, Fang Y, Xiong B. EGCG synergizes the therapeutic effect of cisplatin and oxaliplatin through autophagic pathway in human colorectal cancer cells. Journal of Pharmacol Sci. 2015;128(1):27-34.
19. Duzgun O, Sarici I, Gokcay S, Ates K, Yılmaz M. Effects of nivolumab in peritoneal carcinamatosis of malign melanoma in mouse model. Acta Cir Bras. 2017;32(12):1006-12.
20. Vinoth A, Kowsalya R. Chemopreventive potential of vanillic acid against 7,12-dimethylbenz(a)anthracene-induced hamster buccal pouch carcinogenesis. J Cancer Res Ther. 2018;14(6):1285-90.
21. Silvan S, Manoharan S. Apigenin prevents deregulation in the expression pattern of cell-proliferative, apoptotic, inflammatory and angiogenic markers during 7, 12-dimethylbenz [a] anthracene-induced hamster buccal pouch carcinogenesis. Arch Oral Biol. 2013;58(1):94-101.
22. Faisal M, Abu Bakar M, Sarwar A, Adeel M, Batool F, Malik KI, et al. Depth of invasion (DOI) as a predictor of cervical nodal metastasis and local recurrence in early stage squamous cell carcinoma of oral tongue (ESSCOT). Plos One. 2018;13(8):e0202632.
23. Ishaq S, Kehar S, Zafar S, Hasan S. Correlation of CD24 expression with histological grading and TNM staging of retinoblastoma. Pak J Med Sci. 2016;32(1):160-64.
24. Dobbin Z, Landen C. Isolation and characterization of potential cancer stem cells from solid human tumors—potential applications. Curr Protoc Pharmacol. 2013;63(1):14.28.
25. Han J, Fujisawa T, Husain S, Puri R. Identification and characterization of cancer stem cells in human head and neck squamous cell carcinoma. BMC cancer. 2014;14(1):173.
26. Bruna F, Rodríguez M, Plaza A, Espinoza I, Conget P. The administration of multipotent stromal cells at precancerous stage precludes tumor growth and epithelial dedifferentiation of oral squamous cell carcinoma. Stem Cell Res. 2017;18:5-13.
27. Kaza S, Kantheti L, Poosarla C, Gontu S, Kattappagari K, Baddam V. A study on the expression of CD44 adhesion molecule in oral squamous cell carcinoma and its correlation with tumor histological grading. J Orofac Sci. 2018;10(1):42-49.

28. Andratschke M, Chaubal S, Pauli C, Mack B, Hagedorn H, Wollenberg B. Soluble CD44v6 is not a sensitive tumor marker in patients with head and neck squamous cell cancer. Anticancer Res. 2005;25(4):2821-26.
29. Williams K, Motiani K, Giridhar P, Kasper S. CD44 integrates signaling in normal stem cell, cancer stem cell and (pre) metastatic niches. Exp Biol Med. 2013;238(3):324-38.
30. AbdulMajeed A, Dalley A, Farah C. Putative cancer stem cell marker expression in oral epithelial dysplasia and squamous cell carcinoma. J Oral Pathol Med. 2013;42(10):755-60.
31. Weichert W, Denkert C, Burkhardt M, Gansukh T, Bellach J, Altevogt P, et al. Cytoplasmic CD24 expression in colorectal cancer independently correlates with shortened patient survival. Clin Cancer Res. 2005;11(18):6574-81.
32. El-Hossary W, Hegazy E, El-Mansy M. Topical chemopreventive effect of thymoquinone versus thymoquinone loaded on gold nanoparticles on dmba-induced hamster buccal pouch carcinogenesis (immunohistochemical study). Egypt Dent J. 2018;64(4):3523-33.
33. Balakrishnan S, Manoharan S, Alias L, Nirmal M. Effect of curcumin and ferulic acid on modulation of expression pattern of p53 and bcl-2 proteins in 7, 12-dimethylbenz [] anthracene-induced hamster buccal pouch carcinogenesis. Indian J Biochem Biophys. 2010;47(1):7-12.
34. Hussein A, El-Sheikh S, Darwish Z, Hussein K, Gaafar A. Effect of genistein and oxaliplatin on cancer stem cells in oral squamous cell carcinoma: an experimental study. Alex Dent J. 2018;43(1):117-23.
35. Paulis Y, Huijbers E, Schaft D, Soetekouw P, Pauwels P, Heijnen V, et al. CD44 enhances tumor aggressiveness by promoting tumor cell plasticity. Oncotarget. 2015;6(23):19634-46.
36. Mărgăritescu C, Pirici D, Simionescu C, Stepan A. The utility of CD44, CD117 and CD133 in identification of cancer stem cells (CSC) in oral squamous cell carcinomas (OSCC). Rom J Morphol Embryol. 2011;52(3):985-93.
37. Fugle C, Zhang Y, Hong F, Sun S, Westwater C, Rachidi S, et al. CD24 blunts oral squamous cancer development and dampens the functional expansion of myeloid-derived suppressor cells. Oncoimmunology. 2016;5(10):e1226719.
38. Rizk O, Elsaka A, Elguindy D. Immunohistochemical study of CD44 and CD24 as cancer stem cell markers and their prognostic role in invasive ductal carcinoma of the breast. Egypt J Pathol. 2016;36(2):235-40.
39. Yang C, Wang H, Lin Y, Kumar K, Lin H, Chang C, et al. Identification of CD24 as a cancer stem cell marker in human nasopharyngeal carcinoma. Plos One. 2014;9(6):e99412.
40. Ghuwalewala S, Ghatak D, Das P, Dey S, Sarkar S, Alam N, et al. CD44highCD24low molecular signature determines the cancer stem cell and EMT phenotype in oral squamous cell carcinoma. Stem Cell Res. 2016;16(2):405-17.
41. Todoroki K, Ogasawara S, Akiba J, Nakayama M, Naito Y, Seki N, et al. CD44v3+/CD24-cells possess cancer stem cell-like properties in human oral squamous cell carcinoma. Int J Oncol. 2016;48(1):99-109.
42. Chen D, Wang Y. Targeting cancer stem cells in squamous cell carcinoma. Precis clin med. 2019;2(3):152-65.
43. Yoshimura H, Yoshida H, Matsuda S, Ryoke T, Ohta K, Ohmori M, et al. The therapeutic potential of epigallocatechin3gallate against human oral squamous cell carcinoma through inhibition of cell proliferation and induction of apoptosis: In vitro and in vivo murine xenograft study. Mol Med Rep. 2019;20(2):1139-48.
44. Chen P, Chu S, Kuo W, Chou M, Lin J, Hsieh Y. Epigallocatechin-3 gallate inhibits invasion, epithelial– mesenchymal transition, and tumor growth in oral cancer cells. J Agric Food Chem. 2011;59(8):3836-44.
45. Hwang Y, Park K, Chung Y. Epigallocatechin-3 gallate inhibits cancer invasion by repressing functional invadopodia formation in oral squamous cell carcinoma. Eur J Pharmacol. 2013;715(1-3):286-95.
46. Rawangkan A, Wongsirisin P, Namiki K, Iida K, Kobayashi Y, Shimizu Y, et al. Green tea catechin is an alternative immune checkpoint inhibitor that inhibits PD-L1 expression and lung tumor growth. Molecules. 2018;23(8):2071.
47. Chung S, Vadgama J. Curcumin and epigallocatechin gallate inhibit the cancer stem cell phenotype via downregulation of STAT3–NFκB signaling. Anticancer Res. 2015;35(1):39-46.
48. Jiang P, Xu C, Chen L, Chen A, Wu X, Zhou M, et al. EGCG inhibits CSC-like properties through targeting miR-485/CD44 axis in A549-cisplatin resistant cells. Mol carcinog. 2018;57(12):1835-44.
49. Mayr C, Wagner A, Neureiter D, Pichler M, Jakab M, Illig R, et al. The green tea catechin epigallocatechin gallate induces cell cycle arrest and shows potential synergism with cisplatin in biliary tract cancer cells. BMC Complement Altern Med. 2015;15(1):194.

50. Mirhashemi M, Ghazi N, Saghravanian N, Taghipour A, Mohajertehran F. Evaluation of CD24 and CD44 as cancer stem cell markers in squamous cell carcinoma and epithelial dysplasia of the oral cavity by q-RT-PCR. Dent Res J. 2020;17(3):208-12.
51. Wang Z, Wang Q, Wang Q, Wang Y, Chen J. Prognostic significance of CD24 and CD44 in breast cancer: a meta-analysis. Int J Biol Markers. 2017;32(1):75-82.
52. Pan X, Zhao B, Song Z, Han S, Wang M. Estrogen receptor-α36 is involved in epigallocatechin-3-gallate induced growth inhibition of ER-negative breast cancer stem/progenitor cells. J Pharmacol Sci. 2016;130(2):85-93.
53. Kumazoe M, Takai M, Hiroi S, Takeuchi C, Yamanouchi M, Nojiri T, et al. PDE3 inhibitor and EGCG combination treatment suppress cancer stem cell properties in pancreatic ductal adenocarcinoma. Sci Rep. 2017;7(1):1917.
54. Chen D, Pamu S, Cui Q, Chan T, Dou Q. Novel epigallocatechin gallate (EGCG) analogs activate AMP-activated protein kinase pathway and target cancer stem cells. Bioorg Med Chem. 2012;20(9):3031-37.
55. Lee S, Nam H, Kang H, Kwon H, Lim Y. Epigallocatechin-3-gallate attenuates head and neck cancer stem cell traits through suppression of Notch pathway. Eur J Cancer. 2013;49(15):3210-18.
56. Kang S, Lee S, Lee H, Baek S, Shin Y, Kim H. Expression of NSAID-activated gene-1 by EGCG in head and neck cancer: involvement of ATM-dependent p53 expression. J Nutr Biochemi. 2013;24(6):986-99.
57. Negri A, Naponelli V, Rizzi F, Bettuzzi S. Molecular targets of epigallocatechin—Gallate (EGCG): A special focus on signal transduction and cancer. Nutrients. 2018;10(12):1936.